Solid state reactions at metal/film interfaces: The case of the Pb/PbSO$_4$ interface☆

C.V. D'Alkaine [a,*], L.L.M. de Souza [b], G.A. de O. Brito [c]

[a] Group of Electrochemistry and Polymers, Chemistry Dep., Federal University of São Carlos, Rodovia Washington Luís, km 235 – SP-310, Caixa Postal 676, São Carlos, São Paulo, CEP 13565-905, Brazil
[b] Energy Accumulator Laboratory, SENAI, Virgílio Malta Street, 11-22, Bauru, São Paulo, CEP 17015-220, Brazil
[c] Agrarian Sciences Center, Federal University of Espírito Santo, Alto Universitário, Caixa Postal 16, Guararema, Alegre, Espírito Santo, CEP 29500-000, Brazil

ABSTRACT

On the base of an analysis of some literature is shown that a solid state reaction mechanism can have several advantages over a dissolution–precipitation mechanism as the most convenient way to describe the Pb/H$_2$SO$_4$ interface in the PbSO$_4$ region, at least for some of the possible experimental conditions. In support of this view, quantitative analyses of the voltammetric results for the formation and reduction of PbSO$_4$ are presented, showing that it is possible to obtain the kinetic parameters of the reactions occurring at the Pb/PbSO$_4$ interface. From these analyses, it is possible to gain a deeper understanding of how the negative plates of lead acid batteries operate efficiently.

© 2012 Elsevier B.V. All rights reserved.

1. Introduction

An understanding of the mechanistic process of lead acid batteries requires an explanation of how they can be discharged and recharged through a large number of cycles. As the battery is discharged, the active electrochemical surface of the plates is chemically altered. To retain the battery's original capacity and structure, these active materials must be completely recuperated in its original state during the charging process.

The prevailing explanation of the charge/discharge processes relates only to a dissolution–precipitation mechanism. This mechanism implies the need for extended relaxation times and the passage of species through a solution that leads to some form of loss of the system's structural memory giving rise to one of the phenomena that can produce the end of cycling under some operational conditions. On the other hand, if a continuous solid state reaction mechanism is partially assumed, the structural memory of the system can be maintained.

The reason of dissolution–precipitation mechanism to be so extensively accepted can be based on Scanning Electron Microscopy (SEM) observations of crystals developed during discharge, which seems to confirm this explanation. In contrast, studies on passivity films during the last fifty years [1] have shown the possibility of film formation through solid state reaction mechanisms under a high electrical field giving rise up to a double-film structure (a internally glued film on the substrate and an external, disrupted film connected to the first film by surface tension). The present paper will try to call the attention to these glued films. Formation of this double film depends on the growth conditions. The solid state reaction mechanism has been validated for the transient initial conditions [2] for very thin nanometric films in which, after an initial growth, the partial disruption of the film follows (in voltammetric, potentiostatic or galvanostatic experiments). It has also been validated for quasi-stationary situations [3].

Studies performed on metals during the last decades using in situ Atomic Force Microscopy (AFM) during voltammetry experiments at low sweep velocities (which make them equivalent to potentiostatic growth) have shown that in solutions in which the electrochemical products are insoluble, a continuous film formed in situ seems to initially cover the substrate. One of these cases (relevant to the work presented here because it refers to lead in sulphuric acid) is found in the paper of Vermesan et al. [4]. If we look at the micrographs' background, increasing the magnification of the micrographs (inside the limits of the technique), it is possible to observe in some of the micrographs of this paper a continuous film and its disruption process.

The present paper, takes into account the above facts to show how, through a continuous solid state film growth model, the voltammetric growth of PbSO$_4$ on Pb and its reduction in an H$_2$SO$_4$ solution can be quantitatively interpreted to obtain the parametric values for the oxidation and reduction reactions at the Pb/PbSO$_4$ interface. These measurements allow for an understanding of the

reactions at this interface in a method similar to that traditionally used for electrochemical reactions at inert electrodes with the oxidised and reduced species in solution when they present ohmic drops.

1.1. Some studies of the Pb/PbSO₄/H₂SO₄ case

To understand the negative plate charge and discharge mechanisms of a lead acid battery, it is important to study flat electrodes in which the electrode reactions are not complicated by the pore structures of the active material, in this case, the spongy Pb. In this section we would like to analyse in this last sense some published papers which are important for the present work.

Studies of rotating disk-ring (RDR) electrodes [5] have shown that, even when there is some dissolution—primarily at the beginning of the PbSO₄ film formation—it never rises above 10% of the total film charge density. Therefore, the fundamental film formation mechanism cannot be as unique process the dissolution–precipitation mechanism in these experiments. To obtain this value of 10% it was necessary to calculate the dissolved charge at the disk from the charge detected at the ring in the referred paper. These calculations have not been made in the referenced paper despite the fact that the authors provide the necessary data. However, the authors agree that the fundamental mechanism cannot be a dissolution–precipitation one.

More recently, in situ AFM has shown [6] that the crystals observed by SEM are completely different from those seen by in situ AFM. Micrographs from both techniques are shown in the referenced paper. The authors observe the electrode after a long period of potentiostatic expositions (on the order of minutes) and propose a model for the growth of the film observed on the metal. Perhaps, the SEM-observed crystals are due to the fact that SEM measurements are ex situ; crystals would be produced on the electrode by the corrosion process during the withdrawal of the electrode from the solution and its subsequent drying if care is not taken [7].

Voltammetric measurements only allow for the observation of the reduction of the glued film on the metal because it is only to this film that high electrical fields can be applied and used to promote reduction within the time scale of a voltammetry experiment and this fact on the reduction processes is a demonstration of the presence of a glued film. The externally disrupted films, pointed out in the first part of this introduction, can only be reduced by a dissolution process of the disrupted particles, followed by the diffusion and precipitation of the cations at the metal surface, requiring longer relaxation times than are afforded by the used voltammetric time scales. For this reason, at the Pb/PbSO₄/H₂SO₄ interface, the voltammetric anodic charge densities are always higher than the cathodic ones giving a clear demonstration of the disruption phenomena of the films. These phenomena have been discussed in detail in a previous paper [2].

1.2. The present voltammetric studies

Taking into account all of the above facts, the present paper reports on the voltammetric quantitative studies of the oxidation and reduction mechanisms at the Pb/PbSO₄ interface in the PbSO₄ potential region without having the idea that the presented description can be extended to any experimental condition, specially if it occurs on the surface of a pore where there can be decrease of acid concentration during film formation.

Following a previous paper in which on flat electrodes nucleation was shown to occur only in the initial stages of the voltammetric peak [8], once the film nucleation has occurred, the system would be considered to be a continuous film. Nevertheless, in order to achieve this situation, at a reasonable initial cathodic potential (E_i), a continuous, very thin nanometric PbSO₄ film was
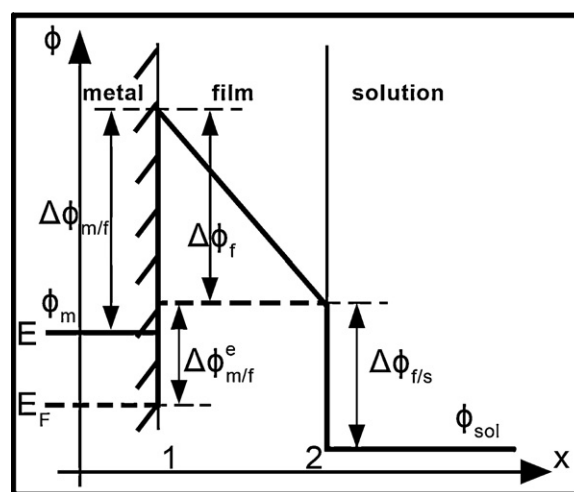

Fig. 1. Variation of the inner potential at a metal/glued film/solution interface. Two cases: (a) growing film at E (continuous line) and (b) stationary film at the Flade potential (dashed line). In the figure the non adherent disrupted film has not been taken into account.

initially grown in each voltammetric experiment of this paper. Under these conditions, the growth of the film can be considered to be the result of a solid state growth mechanism in a high electrical field.

In contrast, for the film reduction studies, after consistently growing the same film that suffers the partial disruption process [2], reduction can only occur in the remaining attached film. Under these circumstances, it is only the remaining film glued onto the metal surface that can be directly reduced by a solid state high electrical field mechanism within the voltammetric sweep time scales. In this sense, for modelling the reduction reactions, the reduced film detected by the voltammetric experiments can be considered also a continuous film attached to the metal.

1.3. The model used [9]

1.3.1. The anodic case

If the film that is adhered to the metal is continuous, it is possible to develop a general differential equation for its growth or reduction [9]. The inner potential differences, $\Delta\phi$, at the metal/film interface (m/f), at the film (f) and at the film/solution interface (f/s) must be considered as given in Fig. 1 for the adhered portion of the film. This is shown in the figure for a potential, E (shown by a continuous curve), with a circulating current density, i, and for E_F, the Flade potential ($i = 0$, shown by the dashed curve). As a consequence, three overpotentials can be defined: the metal/film overpotential ($\eta_{m/f}$), the film overpotential (η_f) and the film/solution overpotential ($\eta_{f/s}$). These overpotentials can generally be defined by the following equation:

$$\eta_j = [\Delta\phi_j(i \neq 0) - \Delta\phi_i^{eq}(i = 0)] \tag{1}$$

in which $\Delta\phi_j^{eq}(i = 0)$ is the equilibrium inner potential difference, and $\Delta\phi_j(i \neq 0)$ is the inner potential difference when the system is not at equilibrium (i.e., when the system has a current density other than zero). Both $\Delta\phi$ values are for the j interface. In any experiment in which there is no significant dissolution of the film, and in following Gerischer [10], when the surface pH for an oxide is maintained at a constant value (in the present case instead the pH, the SO₄²⁻ surface concentration), the $\eta_{f/s}$ can be considered constant and incorporated into E_F. This is the reason why Flade potentials of oxides are pH dependent, and, in the present case, the Pb/PbSO₄/H₂SO₄ reversible potential is sulphuric acid dependent. Therefore, during a voltammetry experiment in a non-dissolving

solution and where the constant $\eta_{f/s}$ can be incorporated to E_F, the following is valid:

$$E(\text{at } i) = E_F(i = 0) + \eta_{m/f} + \eta_f$$

or $\quad \eta_T = \eta_{m/f} + \eta_f = E(\text{at } i) - E_F(i = 0)$ \hfill (2)

in which η_T is the total overpotential.

It has been shown [9] that, just as any continuous film model must follow the same differential equation, there is a general correlation between the overpotential at the voltammetric peak and the experimental variables given by the following equation:

$$\eta_{f,p} = \frac{\nu \times q_{p,a}}{i_{p,a}}$$ \hfill (3)

in which the sub-index, p, denotes the peak condition; ν, the voltammetric sweep rate; and $q_{p,a}$ and $i_{p,a}$, the anodic peak charge density and current density, respectively. Knowing the voltammetries at different values of ν, $q_{p,a}$, and $i_{p,a}$, it is then possible to calculate the corresponding anodic film peak overpotentials, $\eta_{f,p,a}$, for each potential sweep rate. As the peak potential ($E_{p,a}$) at each value of ν can also be experimentally determined, calculating the $\eta_{f,p,a}$ at different ν (using Eq. (3)), the film ohmic correction can be applied to $E_{p,a}$ at different ν. As a consequence, it is possible to plot the natural logarithm of the current density at the anodic peak, $\ln i_{p,a}$, versus the corrected peak potential for the ohmic drop through the film, $(E_{p,a} - \eta_{f,p,a})$, as is normally done for electrochemical reactions in solution when there is an ohmic drop. Nevertheless, in the present case the corresponding reaction is a solid state oxidation reaction at the metal/film interface and can be described in our case by the following:

$$Pb^{2+}(\text{on the metal surface}) \Rightarrow Pb^{2+}(\text{interstitial position in the film}) \quad (4)$$
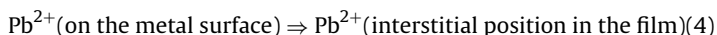
In Eq. (4) the end product is considered to be Pb^{2+} in an interstitial position of the film. The original thin continuous film, formed at the initial potential, E_i, is considered to be very thin, and consequently, presents very low levels of cation vacancies to permit the incorporation into them of the Pb^{2+} ions.

If the activated energy barrier of the process corresponding to Eq. (4) is symmetric, the anodic transfer coefficient (α_a) of this reaction must be 1.0. The amount of charge transferred up to the activated complex will be 1.0 for a 2+ cation. This can be tested in the experimental data, and if the correct procedures are followed, the plot will yield something equivalent to the well-known Tafel plots for reactions in solution, proving that the previously stated considerations can be taken as a reasonable description of the process.

1.3.2. The cathodic case

To study the reduction reaction, it is convenient to first grow the same film for each measurement, voltammetrically plus potentiostatically, to arrive at the same formation charge density before the reduction. In the present case the thickness of the film grown before the reduction was always equivalent to 57 mC cm^{-2}. It was then possible to apply the same considerations and equations used in the voltammetric oxidation case to the voltammetric reduction. Nevertheless, for a reduction peak, when the current arrives at the peak, the film through which the current density is passing is the film remaining at the cathodic peak (the remaining or remanescent cathodic charge density, $q_{p,rem,c}$, see Fig. 2). It is this remaining charge density, together with the corresponding values of ν_c and $i_{p,c}$, that must now be used in Eq. (3). If the cathodic peak, $E_{p,c}$ is corrected for the remaining cathodic film overpotential ($\eta_{f,p,rem}$) through the film at the cathodic peak, $(E_{p,c} - \eta_{f,p,rem})$, we would obtain the Tafel plot of the solid state reduction reaction at the corresponding metal/film interface. Therefore, the plot of $\ln i_{c,p}$, versus $(E_{p,c} - \eta_{f,p,rem})$ must, once again, yield a typical Tafel plot with a
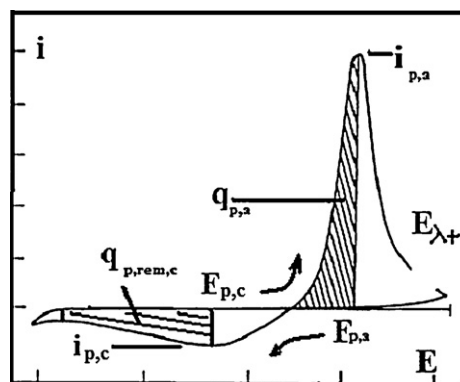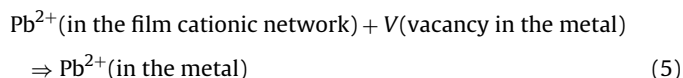

Fig. 2. Voltammetric anodic/cathodic curves for the Pb/PbSO$_4$/H$_2$SO$_4$ system pointing out the different used parameters.

cathodic transfer coefficient, α_c, given by $(2 - \alpha_a)$. The reduction data would also support the above analysis. The solid state reaction in the reduction case can be described as follows:

$$Pb^{2+}(\text{in the film cationic network}) + V(\text{vacancy in the metal})$$

$$\Rightarrow Pb^{2+}(\text{in the metal}) \hfill (5)$$

The vacancies near the surface of the metal are produced by the oxidation reaction during the previous film formation.

2. Experimental

The electrodes were flat surface of 99.99% pure Pb bare, which was included in an epoxy resin inside a glass tube and with only one Pb circular free face polished with 600 grit emery paper, washed and dried with an absorbent paper before each voltammetric measurement. The solution was an unvarying 4.6 M H$_2$SO$_4$ always de-oxygenated. The reference electrode was a normal Hg/Hg$_2$SO$_4$/H$_2$SO$_4$ (4.6 M) with its capillary tip immersed in the working solution in front of the working electrode. The counter electrode was a Pt disk located in the electrochemical cell in front of the Pb surface. The initial potential, E_i, for the anodic voltammetric growth was a constant -1.2 V where it was waited up to a stationary current density. The anodic (ν_a) or cathodic (ν_c) sweep potential rates are given in the figures.

For the reduction process, the film was first at each time grown sweeping at 10 mV s^{-1} the electrode from $E_i = -1.2$ V to a growing potential $E_g = -0.96$ V (at the beginning of the anodic peak region). This potential was maintained until the passage of a total anodic charge density ($q_{a,T}$) of 57 mC cm^{-2}, which included the charge density that passed during the voltammetry and at E_i.

Fig. 2 shows a general view of an anodic and a cathodic voltammetry experiment without any anodic growing stop. This figure points out the different parameters that will be used: current density, i; anodic ($i_a > 0$) and cathodic ($i_c < 0$) current densities; voltammetric anodic and cathodic peak potentials, $E_{p,a}$ and $E_{p,c}$; anodic peak charge density and remaining cathodic peak charge density, $q_{p,a}$ and $q_{p,c,rem}$, respectively; and the limit maximum sweep potential, $E_{\lambda+}$.

3. Results and discussion

3.1. The anodic case

Fig. 3 shows the general trend in the values of the anodic voltammetric results with varying ν_a. It is from this data that the calculations of the anodic case were made.
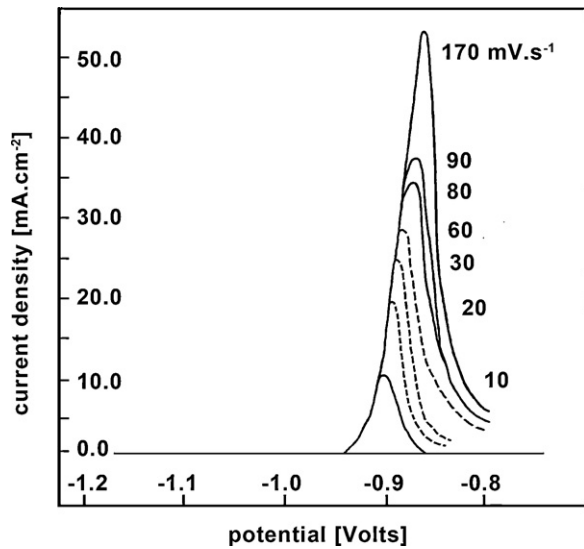
Fig. 3. First anodic voltammetric sweeps at different rates for the growth of the PbSO$_4$ film on Pb in a 4.6 M H$_2$SO$_4$ solution. RE Hg/Hg$_2$SO$_4$/H$_2$SO$_4$ (4.6 M) solution.

From the data in Fig. 3, the anodic peak current densities ($i_{p,a}$) versus the square root of the varying sweep rates (v_a) has been plotted in Fig. 4. The relationship between these two variables must follow the equation below [9] for a solid state ohmic growth mechanism:

$$i_p = \frac{1}{(V_f \rho_f)^{1/2}} v_a^{1/2} \tag{6}$$

V_f is the volume per coulomb of the growing film, and ρ_f is its ionic resistivity. In general, ρ_f can vary under transient conditions.

V_f is generally constant; it does not change very much even from one film to another. The loss of linearity at low v_a in Fig. 4 can be attributed to a variation in ρ_f with aging. The figure also shows at sweep rates higher than approximately 50 mV s^{-1} a constant ionic specific resistivity of $2.51 \times 10^4\ \Omega$ cm (considering a V_f for the PbSO$_4$ film equal to 2.53×10^{-4} cm^3 C^{-1}). A growing sweep region at low sweep rates in which the ρ_f increases with decreasing v_a shows the presence of an aging phenomenon when the slow-growing process allows time for aging. These results are in agreement with those of passivating films [9]. In contrast, the PbSO$_4$ films present ionic resistivity 10^2–10^3 times lower than that of
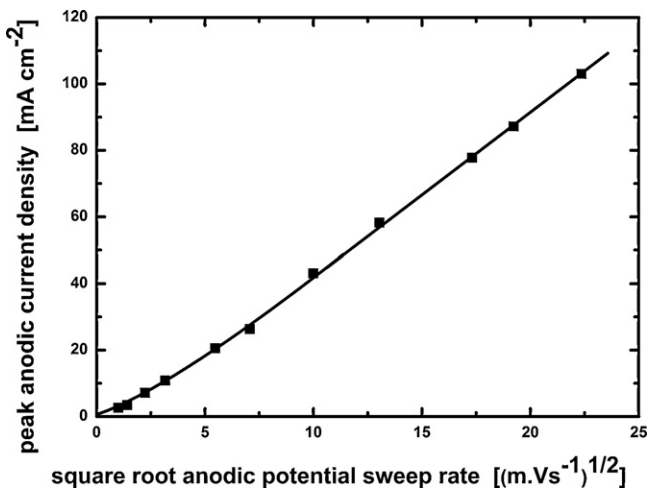

Fig. 4. Plot of the anodic peak current density vs. square root of the anodic potential sweep rate.
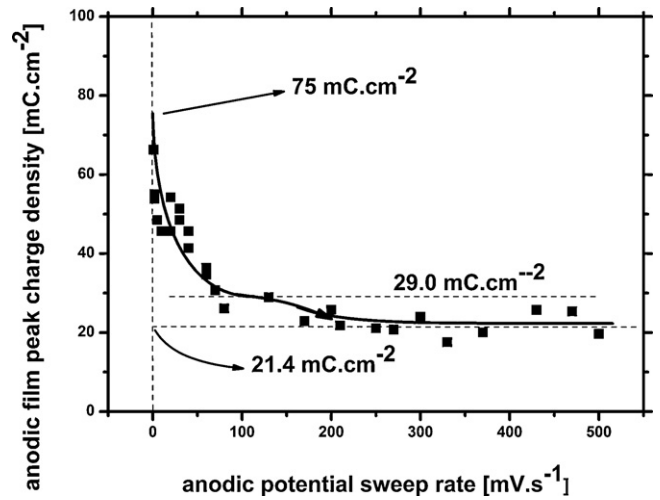Data from Fig. 3.

Fig. 5. Plot of the anodic peak charge density vs. the anodic potential sweep rate. Obtained from Fig. 3.

the normal passivating films. Therefore, the PbSO$_4$ films become thicker than normal passivating films and can serve as a good negative electrode for the lead acid battery, especially if a highly active electrochemical area is added via the macro- and microporosity of the plates.

The presence of a continuous film can also be confirmed by the plot of the charge density versus the sweep as shown in Fig. 5.

In Fig. 5, two constant charge density levels are seen, one yielding 21.4 mC cm^{-2} at high v_a and the other yielding 29.0 mC cm^{-2} at intermediate v_a. These two levels indicate two stationary states in relation to the growing rate (v_a), pointing to the possible existence of two types of PbSO$_4$ films. The important aspect from the point of view of the present paper is that the decrease in the anodic charge density shown in Fig. 5 (ignoring the level at the intermediate v_a) is generally found in passivating films studies [9], and the tendency towards a low constant charge density at high v_a is related to the growing process of the film at high sweep rates [2].

Finally, using Eq. (6) and knowing the values of v_a, $i_{p,a}$ (Fig. 4), and $q_{f,a,p}$ (Fig. 5), it is possible to calculate $\eta_{f,a,p}$. With these values and the anodic peak potential (from Fig. 3), it will be possible to calculate the potential corrected for the ohmic drop through the film, meaning the potential at the Pb/PbSO$_4$ interface, which must yield a Tafel relationship if all analyses are correct.

Nevertheless, there is still one problem: the voltammetric film peak charge density ($q_{f,p,\text{volt}}$) is not the complete film charge density because at the initial potential, E_i (in our case -1.2 V), some monolayers of PbSO$_4$ film with an initial charge density, q_0, have been grown. Ignoring this fact yields non-linear regions in the Tafel plots, but simultaneously provides a method to estimate the value of q_0. Actually, the quantity q_f is given by the following equation:

$$q_{f,p,a} = q_0 + \frac{1}{v_a} \int_{E_i}^{E_{p,a}} i_a\ dE \tag{7}$$

in which $E_{p,a}$ is the peak potential at v_a.

The method to determine q_0 is based on the fact that in the calculations of $q_{f,a,p}$, as q_0 is increased, the original curve of $\ln i_{p,a}$ versus ($E_{p,a} - \eta_{f,p,a}$) with $q_0 = 0$ becomes linearised at high i_a. If to q_0 is given a low value, there is no linearization of the plot. If to q_0 is given a very high value, at high i_a, the curve shifts to the left as $\ln i_{a,p}$ increases, which is unacceptable. Following the evolution of the plot of $\ln i_{p,a}$ versus ($E_{p,a} - \eta_{f,p,a}$), calculating $\eta_{f,p,a}$ for different attributed values of q_0, it is possible to determine, recursively, the true q_0 value for any selected E_i. In our case, for an E_i value of
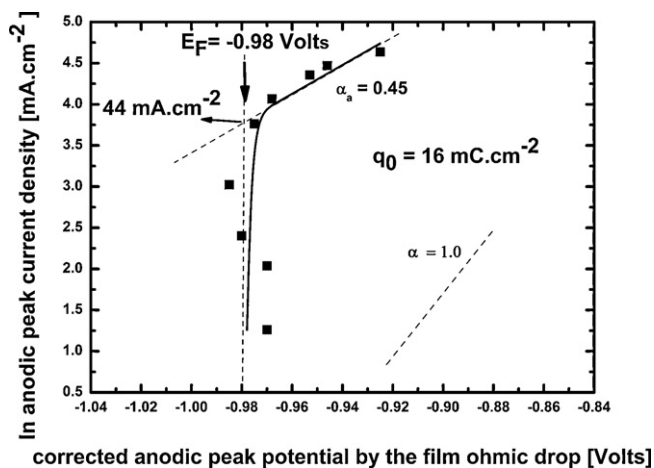
Fig. 6. Tafel plot of the natural logarithm of the anodic current density versus the corrected peak potential for the ohmic drop through the film at the Pb/PbSO$_4$ interface.

-1.2 V, a q_0 value of 16 mC cm^{-2} was obtained. This value was used to calculate the $q_{f,p,a}$ values and to construct Fig. 6.

This figure shows a typical Tafel plot in which, for low i, the cathodic (or reverse) current density of the process develops, and the plot's linearity is lost. For the linear region, $i_a \gg i_c$, if the process is a simple one-step activated process, the tangent must be given by $1/\alpha_a f$ (with $f = F/RT$, and α_a being the anodic charge transfer coefficient). From this it is possible to calculate α_a, in the present case 0.45. A related total charge transfer of 2 (transfer of Pb^{2+} ions, Eq. (4)) should yield a value of $\alpha_a = 1.0$ if the activated complex barrier was symmetric. A value of 0.45 indicates that the barrier is deformed, with a maximum near the metal. This finding implies that the free energy wall for the Pb^{2+} ions is deeper in the metal side than in the interstitial position of the PbSO$_4$ film. The finding is in agreement with the fact that the reaction product is an interstitial cation, and the film, created at high sweep rates (high i), is a non-aged film. In contrast, the Flade potential, E_F, is determined as i becomes zero (the ln i becomes $-\infty$); it is possible then to estimate the value of E_F using Fig. 6. The resulting value for the oxidation process was $E_F = -0.98$ V. This is in reasonable agreement with the reversible potential of the system even though the value is coming from a kinetic point of view. Finally, knowing E_F and extrapolating the linear anodic region of the Tafel plot, it is possible to determine the exchange current density of the process (i^0) which was found to be 44 mA cm^{-2}. This value provides another explanation for the efficiency of the system as a battery plate: it has a very high exchange current density at the Pb/PbSO$_4$ interface. These facts together point to the description of the discharge process of negative plates as a solid state reaction, giving rise to a continuous film that can suffer disruption. This result leads to a deeper understand of the operation characteristics of the lead acid battery system.

3.2. The cathodic case

Fig. 7 shows the reduction voltammetries following the growth of the PbSO$_4$ film voltammetrically and potentiostatically up to always a film charge density of $q_{f,a} = 57$ mC cm^{-2}.

The cathodic peak current density ($i_{p,c}$) versus the square root of the sweep rates are presented in Fig. 8 to confirm whether or not the data follow Eq. (6) (in which ν_a is replaced by ν_c).

In contrast to the anodic case shown in Fig. 4, Fig. 8 illustrates that linearity is obtained for low sweep rates and that departure from linearity occurs at high sweep rates. This is in agreement with the presented theory if, in the reduction case, the reduced film is
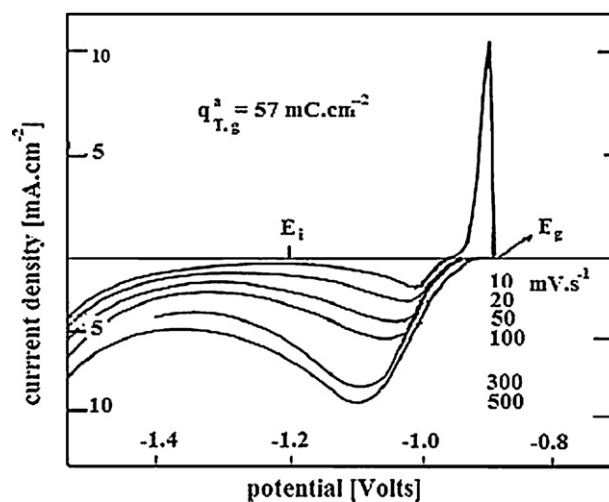

Fig. 7. Voltammetric reductions of a constant PbSO$_4$ film (57 mC cm^{-2}) at different potential sweep rates. E_i is the initial potential before the anodic voltammetry; E_g is the potentiostatic growing potential following the anodic sweep from E_i up to E_g, before the reduction voltammetry. Each reduction voltammetry corresponds to the growth of one specific film.

considered an aged film, and at low rates, the passing current densities are too low to modify the initial aged film via the injection of point defects. Nevertheless, at high sweep rates the current densities become significant enough to modify the film's ionic resistivity. In the present case the film's ionic resistivity becomes higher (Eq. (6), at the peak conditions), demonstrating that, as the films become thinner (see Fig. 9), the point defects recombination becomes faster than the injection. It must be remembered that the reduced films have suffered the disruption process causing them to become even thinner (see the values of $q_{p,rem,c}$ in Fig. 9 as compared with the total anodic film charge density, 57 mC cm^{-2}).

Another important finding in Fig. 8 can be seen in the extrapolation of $i_{p,c}$ to $\nu^{1/2} = 0$. The extrapolated line passes through zero showing that at this level of detection there is practically no dissolution current density.

Fig. 9, also derived from the data in Fig. 7, presents the relationship between changes in the cathodic remaining peak charge density (the film thickness at the cathodic peak conditions) and the reduction sweep rate (ν_c). It is necessary to point out that, as the reduction peak is only a part of the total formed film (always
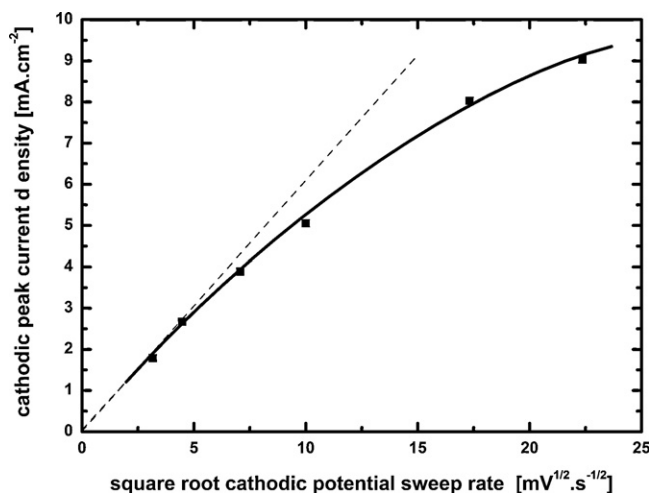

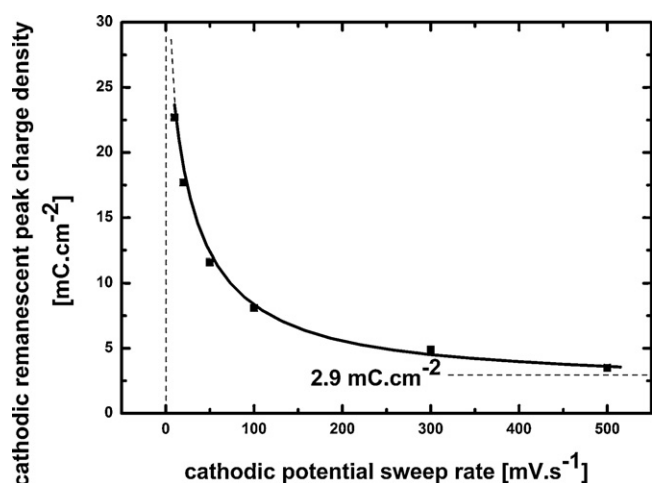**Fig. 8.** Cathodic peak current density versus the square root of the sweep rate. Data from Fig. 7.
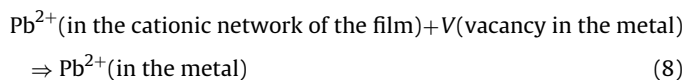
Fig. 9. Cathodic peak remaining charge density versus the sweep rate Data obtained from Fig. 7.
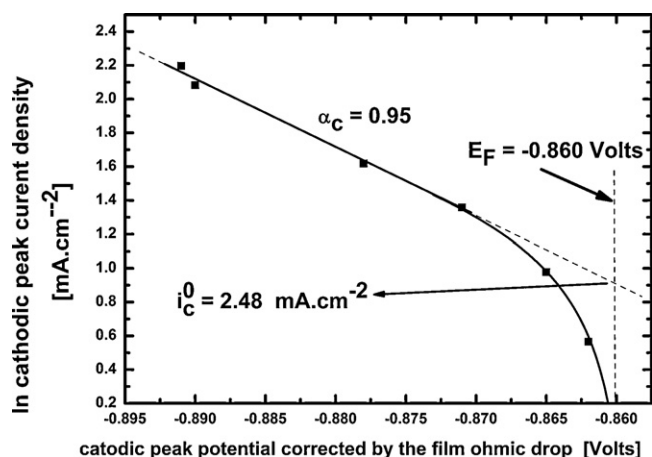

Fig. 10. Plot of the natural logarithm of the cathodic peak current density versus the cathodic peak potential corrected for the ohmic drop through the cathodic remaining film at the peak, calculated using Eq. (3). α_c, cathodic transfer coefficient, i^0, cathodic exchange current density, both at the Pb/PbSO$_4$ interface; E_F, Flade potential.

57 mC cm^{-2}), there is a disruption of the film, and the cathodic voltammetry only detects the remaining film glued on the metal. The electrical field can only be applied to this film for its reduction. The disrupted part of the film must be reduced through a dissolution–precipitation mechanism [2] requiring longer times than the voltammetric ones.

From Fig. 9 it is possible to see that for high sweep rates the $q_{c,p,rem}$ tends towards a constant minimum value (in this case, 2.9 mC cm^{-2}). The value for the corresponding total remaining cathodic charge density ($q_{c,T,rem}$) was 7.2 mC cm^{-2}. The phenomenon indicates that there is a part of the film that it is never disrupted at the high sweep rates of the voltammetries [2]. Simultaneously, these findings may indicate the influence of a hydrogen evolution reaction occurring through the remaining film under the given conditions. In fact, we are presently studying the constant charge density at high reduction sweep rates, which we predict will be dependent on the solution composition [2].

Knowing $i_{c,p}$ and $q_{c,p,rem}$, and using Eq. (3), it is then possible to calculate $\eta_{c,p,rem}$, the overpotential through the cathodic remaining film at the cathodic peak. Note that in Eq. (7), applied now to the reduction case, there is no q_0 and the integration must be made from the cathodic peak (E_p) up to the end of the peak taking into account only the cathodic reduction currents of the remaining film (eliminating the hydrogen reduction current density). Having $\eta_{c,p,rem}$ for each v_c and $E_{c,p}$ it is now possible to correct $E_{c,p}$ for the ohmic drop through the film (as was done in the anodic case), and to make possible the plot of $\ln i_{c,p}$ versus $(E_{c,p} - \eta_{c,p,rem})$, which must yield (as in the anodic case) a Tafel representation if all previous suppositions are correct. A plot of these results is shown in Fig. 10. The process following a one-step mechanism can now be represented by the following equation:

Pb^{2+}(in the cationic network of the film)$+V$(vacancy in the metal)

$$\Rightarrow \text{Pb}^{2+}\text{(in the metal)} \qquad (8)$$

If this reaction has a symmetrical activated complex barrier, it must yield a cathodic transfer coefficient, α_c, of 1.0 for a 2+ ion. Fig. 10 shows that α_c had a value of 0.95 with an E_F of -0.860 V.

The fact that E_F in this experiment is higher than in the anodic experiments (-0.980 V, see Fig. 6) is related to the fact that in the reduction case we are looking at an aged film with fewer point defects. This fact also confirms the deviation of α_a (the anodic result) from 1.0 to 0.45 (see Fig. 6) because the reaction

product was at an interstitial position in a non-aged film. Finally, the obtained cathodic exchange current density, i^0, was found to be 2.48 mA cm^{-2} as compared with 46 mA cm^{-2} for the anodic case (see Fig. 6). This finding is also in agreement with the fact that the reduction experiments are related to aged films.

All of this evidence supports the proposed interpretation and provides new validation for the proposed ideas. More importantly, the given data and their interpretation can lead to a deeper understanding of the charging/discharging processes of the negative plates in lead acid batteries.

4. Conclusions

It is supposed in the case of Pb flat electrodes in H$_2$SO$_4$ that films oxidised or reduced during voltammetric experiments can be partially seen as a continuously attached to the metal surface, even though during the reduction the glued part can suffer partial disruption. This supposition has been used to describe quantitatively the oxidation and reduction mechanisms of lead at the Pb/PbSO$_4$ interface. At the same time, the proposed hypotheses have permitted an understanding of several aspects of the voltammetric results at the Pb/PbSO$_4$ interface. All of these results validate the hypothesis and permit a deeper understanding of the operation of the negative plates in lead acid batteries.

References

[1] Ph. Marcus e V. Maurice (Ed.), Passivation of Metals and Semiconductors and Properties of Thin Oxide Layers, Elsevier, Amsterdam, 2006.
[2] C.V. D'Alkaine, M.C. Garcia, P.M.M. Pratta, G.A.O. Brito, F.P. Fernandes, J. Solid State Electrochem. 11 (2007) 1575–1583.
[3] D.D. Macdonald, Electrochim. Acta 56 (2011) 1761–1772.
[4] H. Vermesan, N. Hirai, M. Shiota, T. Tanaka, J. Power Sources 133 (2004) 52–58.
[5] F.E. Varela, M.E. Vela, J.R. Vilches, A.J. Arvia, Electrochim. Acta 38 (1993) 1513–1520.
[6] Y. Yamaguchi, M. Shiota, Y. Nakayama, N. Hirai, S. Hara, J. Power Sources 93 (2001) 104–111.
[7] F.P. Fernandes, C.V. D'Alkaine, R.L. Tranquelin, Proceedings IMC17-Internacional Microscopy Congress, Rio de Janeiro, 2010, p. 187 (Internet Access 111-14).
[8] C.V. D'Alkaine, P.M.P. Pratta, in: Ph. Marcus e V. Maurice (Ed.), Passivation of Metals and Semiconductors and Properties of Thin Oxide Layers, Elsevier, Amsterdam, 2006, pp. 161–166.
[9] C.V. D'Alkaine, P.C. Tulio, M.A.C. Berton, Electrochim. Acta 49 (12) (2004) 1989–1997.
[10] H. Gerischer, Electrochim. Acta 34 (1989) 1005–1009.